A Nonequilibrium Molecular Dynamics Simulation of the Time-Dependent Orientational Coupling between Long and Short Chains in a Bimodal Polymer Melt upon Uniaxial Stretching

Sandra Barsky and Gary W. Slater*

Department of Physics, University of Ottawa, 150 Louis-Pasteur, Ottawa, Ontario K1N 6N5, Canada

Received December 16, 1997; Revised Manuscript Received July 12, 1999

ABSTRACT: Orientational coupling mediated by steric effects and relaxation in a pearl necklace model of bidisperse polymer melts is investigated by nonequilibrium molecular dynamics simulation. The melts consist of two lengths of chemically identical polymers, which ranged in size from well below to above the entanglement length. The volume fraction of the short polymer is in the range $0.1 \leq \varphi_S \leq 0.9$. After the imposition of a step strain on the melt, the relaxation of the orientational and conformational properties of both species are monitored. The relaxation properties vary as a function of polymer length and blend composition, consistent with experimental data. The degree of steric interactions is varied by changing the density of the system; as expected, slower relaxation rates result from a greater degree of excluded volume. The orientational coupling parameter ϵ, relating the orientation of the short polymer to that of the long, is measured and is in qualitative agreement with experiment. Finally, the stress−optical law is found to be valid during the relaxation process.

I. Introduction

Orientational correlation in polymer networks has attracted much attention in recent years. The possibility of orientational coupling was first broached by DiMarzio,[1] who examined the effects of excluded volume on the entropy of a lattice model of stretched rubber. He found that it was entropically favorable for a chain in an oriented medium to adopt an orientation consistent with its environment. Since that time, a number of other theoretical approaches have found orientational correlations in polymer networks and melts. A wide variety of experimental techniques have been used to investigate this problem, including fluorescence polarization, small-angle neutron scattering (SANS), deuterium nuclear magnetic resonance (DNMR), infrared dichroism, and depolarized Rayleigh scattering. A typical approach is to embed short polymer probes into an amorphous network and apply a macroscopic deformation (i.e., a step strain). Probe molecules orient in the direction of orientation of the surrounding matrix, even when the probes are too small to be entangled. There are many factors influencing the degree of orientation of the probe chains, among which are the stiffness and length of the probe, monomer size, network extension, and temperature. An excellent review of many experimental findings can be found in Ylitalo et al.[2] Orientational coupling of probe molecules in oriented networks supports the hypothesis that a similar orientation occurs in deformed polymer melts, but in this case the orientation is time-dependent since melts do not support stress indefinitely. Recent experimental evidence on bimodal melts[3−5] indeed indicates that orientation coupling does occur in melts as well. In this paper we review selected experimental and theoretical findings and relate these findings to our extensive computer simulations.

There is a wealth of experimental data examining the issue of orientational coupling in polymeric systems. Many experiments were done on blends of different chemical species, where a short probe molecule of one species is swollen into a network of another species. Although orientational correlations are clearly evident in such systems, differences in monomer size and mobility or different relaxation rates as a function of temperature can lead to difficulty in interpretation of data. To simplify these issues, this overview focuses on experiments where the probe and host chains belong to the same chemical species. Brereton and Ries[6,7] performed NMR studies of free chains in deformed network: the orientation of the free chains was mainly accounted for by isotropic excluded-volume interactions. Sotta et al.[8] labeled short poly(dimethyldiloxane) (PDMS) chains with deuterium and then embedded the chains in an end-linked PDMS network. Orientation is commonly measured as the second Legendre polynomial, or order parameter,

$$Q \equiv P_2(\cos(\vartheta)) = \frac{3\langle\cos^2(\vartheta)\rangle - 1}{2} \qquad (1)$$

where ϑ is the angle between the bond and the direction of elongation. After the sample was uniaxially elongated by a factor of up to $\lambda \leq 1.55$, they found that all probe chains acquired a nonzero orientation so long as the network chains remained stretched and that the probe chains were oriented to the same degree as the network chains. This result is in contrast to the classical theory of rubber[9] whereby a chain becomes oriented only by an affine deformation of the junction points. This study clearly shows that orientational coupling exists between the network chains and the free probe chains and that this coupling prevents the relaxation of the probe to an isotropic distribution of bond orientations. As well, since the probe chains were too short to be entangled, this study demonstrates that the coupling is not due to probe entanglement with the host chains. These findings were augmented by examining similar samples with SANS.[10] This technique complements the NMR work since the latter probes on the length scale of a few angstroms (or

* To whom correspondence should be addressed. E-mail: gary@physics.uottawa.ca.

10.1021/ma971826x CCC: $18.00
Published on Web 09/03/1999

a segment length) while SANS probes length scales of 10−100 Å, or about the size of the radius of gyration (R_g) of the polymer. These experiments showed that there was no anisotropy in the orientation of the probe chains, which indicates that the orientation detected at the segment level does not affect the longer length scales. Thus, the interactions leading to such effects must be very local in nature.

The existence of orientational coupling between unattached probe molecules and cross-linked chains in a network suggests that a similar coupling should occur for polymers in a melt. However, the orientational coupling is expected to be time-dependent here since a melt is incapable of sustaining stress after a step strain. Experimentally, orientational coupling in melts was examined by Tassin, Baschwitz, Moise, and Monnerie (TBMM)[5] and Ylitalo et al.[2] for short probe chains in an entangled melt and by Kornfield et al.[3] and Ylitalo, Kornfield, Fuller, and Pearson (YKFP)[4] for fully entangled bidisperse melts. Using infrared dichroism, TBMM studied unentangled polystyrene (PS) probes in PS melts. Uniaxial orientation was achieved by imposing a constant strain rate on samples containing 15 wt % of short, S, polymer in a melt of long, L, polymers until a deformation ratio of $\lambda = 4$ was reached; the relaxation of the polymers was subsequently monitored. In all experiments the relaxation took the form of a fast initial decay of the orientation followed by a very slow decay. The orientation of the L polymer was greater than that of the S polymer, but the S polymers always retained some degree of orientation while the L chains remained oriented. In systems with the longest chains, the relaxation rate of these chains was insensitive to which length of S chain was present. Experiments with different lengths of S chains showed different initial orientations but subsequently showed the same orientation. In YKFP's experiments on fully entangled bimodal melts, birefringence and infrared dichroism were simultaneously measured to evaluate the bulk stress and relaxation, respectively. A primary goal of this work was to measure how the relaxation rates of both long and short polymers varied with volume fraction. To this end, poly(ethylenepropylene) was prepared in three different lengths, which were well beyond the entanglement length. Step strains of up to $\lambda = 1.3$ were imposed on different bimodal melts. In each case, the relaxation times of the orientation of both polymers and of bulk stress decreased with increasing φ_S. The apparent longest relaxation time of L increased with increasing molecular weight and decreasing volume fraction of S. This was interpreted as a clear indication of orientational coupling of the chains to their environment.

Using the above technique, Ylitalo et al.[2] did a systematic study of the effect of the length of the short polymer in a bimodal blend of polybutadiene. The long polymers were fully entangled, while the short ones ranged from well below the entanglement length to well above it, at fixed volume fraction $\varphi_S = 0.2$. When the short polymers are well below the entanglement length, the bulk stress and the relaxation of the long polymer's orientation are nearly identical. As the short polymer increases in length, it makes a greater contribution to the bulk stress.

The main experimental results can thus be summarized as follows. In an oriented medium, short chains remain oriented until the matrix chains are no longer oriented. Short chains are sensitive to their environment in that their degree of orientation and of relaxation are related to how quickly their environment is returning to isotropy.

Various theories are able to predict orientational coupling, either through directly accounting for the effects of excluded volume on entropy, by including a nematic interaction, or by a slight modification of the Doi−Edwards[11] model of reptation. These models will be discussed in turn. As mentioned previously, the first calculation of the effect of orientation on polymer conformations was carried out by DiMarzio.[1] He found that when the system is deformed by a uniaxial stretch, the number of available configurations is changed, thereby enhancing the contribution from the packing entropy arising from excluded-volume effects. That is, in an oriented medium a free chain orients not only due to imposed external stress but also to maximize entropy. A modification of this theory by Tanaka and Allen[12] focused on specific models of random walks. A systematic study of the entropy of different polymer models indicated that for most commonly used models, ranging from freely jointed chains to rigid rods, it was entropically favorable for the polymers to have a residual orientation if the system was even slightly deformed in one direction.[13]

Since steric effects are difficult to introduce in off-lattice models, one way to mimic orientational coupling is through the introduction of phenomenological nematic field terms. In their calculation of the free energy of a polymer, Jarry and Monnerie[14] included a nematic term that was a function of the orientation of the surrounding medium. They found that in an anisotropic medium a flexible test polymer acquires an orientation consistent with the surrounding polymers. A more direct approach was taken by Doi and Watanabe,[15] who included a Maier−Saupe potential in their calculation of the free energy of a freely jointed chain; the rheological properties of a melt undergoing shear deformation were found to be insensitive to the nematic interaction. Nematic terms were also included in two separate reptation-based theories.[16,17] The calculations by Merrill et al.[16] were within the Doi−Edwards framework for reptation,[11] except that when a chain end emerges from the confining tube, its new direction is no longer chosen isotropically, but the direction is chosen to be consistent with the overall orientation. In this way, a polymer becomes partially aligned with the medium. It should be noted that Merrill et al. account for this orientational coupling only through the boundary conditions on the chain ends and not through an imposed nematic interaction.

Another model of orientational coupling in a reptation framework was proposed by Doi et al.,[17] who included an explicit nematic interaction in the calculation of the orientation and the stress. This calculation results in two measures of orientation for a polymer: that of its tube, or primitive path, and that of the actual polymer segments within the tube. Interestingly, this model predicts that the stress−optical law remains valid for a bidisperse blend even in the presence of orientational coupling. As we will see later, our results agree with this prediction.

Gao and Weiner[18] showed the importance of steric effects by computer simulations. Using a truncated Lennard-Jones potential for self-avoidance, they simulated the three-chain model of rubber, in which three chains with different end-to-end distances lie along

three mutually perpendicular directions. They found that fully self-avoiding chains were more oriented than chains with no excluded volume. In subsequent work,[19,20] Gao and Weiner examined the stress of dense polymer melts after a deformation. The dominant contribution to stress was found to originate in interchain excluded-volume interactions. This work thus suggests that steric interactions play a key role in polymer dynamics, as well as in orientational and relaxation processes.

In this paper we report results of extensive computer simulations investigating orientational coupling. We start with equilibrated bimodal polymer melts and perform a step strain which affinely deforms all the polymers. The relaxation of the orientation and conformation of each species as well as the bulk stress is monitored. The polymers range in length from short unentangled chains to entangled melts. We examine the relaxation rates as a function of polymer length, volume fraction, and density of the system and compare with experimental data.

II. The Model

Computer simulations on a broad range of polymer models have shown that many important rheological results can be obtained with models that do not include specific chemical details. The model used in this paper is similar to that used by Kremer and Grest.[21] All monomers in the simulation box interact with the repulsive part of a Lennard-Jones potential

$$U_{\text{rep}}(r_{ij}) = 4\epsilon\left[\left(\frac{\sigma}{r_{ij}}\right)^{12} - \left(\frac{\sigma}{r_{ij}}\right)^{6} + \frac{1}{4}\right] \qquad r_{ij} < 2^{1/6}\sigma$$

$$U_{\text{rep}}(r_{ij}) = 0 \qquad r_{ij} \geq 2^{1/6}\sigma \tag{2}$$

where r_{ij} is the distance between the centers of beads i and j. Note that since the attractive part of the Lennard-Jones potential has been cut off, only interbead steric interactions are present. Neighboring beads along a linear chain are tethered by the anharmonic spring potential

$$U_{\text{T}} = -0.5kR_0^{\,2}\log\left(1 - \frac{r_{ij}^{\,2}}{R_0^{\,2}}\right) \qquad r_{ij} < R_0 \tag{3}$$

where the energy and length parameters are $k = 30\epsilon/\sigma^2$ and $R_0 = 1.5\sigma$, respectively. The (N,V,T) simulations were performed in one of two ways. A constant energy molecular dynamics procedure was used with the equations of motion solved by a velocity Verlet algorithm.[20] The monomers' velocities were rescaled every few integration steps to keep a constant temperature of $k_{\text{B}}T/\epsilon = 1$. The second method consisted of a Brownian dynamics technique[21] where the equations of motion include a term that couples the system to a white-noise source and a heat bath, to maintain the temperature. A detailed comparison of the two methods was made, and the results were indistinguishable. All simulations have periodic boundary conditions, and most of the work is done at a density of $\rho = 0.8$, a system which is known to be a dense melt.[19] The density $\rho = N\sigma^3/V$ where V is the volume.

To examine slightly different polymeric models, two minor changes were made with respect to the above model. First, to explore the effect of steric interactions, two additional system densities (namely, $\rho = 0.4$ and $\rho = 1.0$) were simulated by altering the size of the box. Second, chain flexibility was reduced by introducing a bending energy potential

$$U_{\text{bend}} = k_{\text{bend}}(\cos\vartheta - \cos\vartheta_0) \tag{4}$$

where $\cos(\vartheta)$ is the angle between two consecutive bonds and ϑ_0 is a reference angle. This potential provided a minor or moderate energy cost to bending for $k_{\text{bend}} =$ 0.1 or 0.9, respectively.

Once a monodisperse equilibrated melt is obtained, a fraction of the polymers is cut in order to obtain a bimodal melt of the desired volume fractions of long (L) and short (S) polymers. We have studied combinations of $N_{\text{S}} = 10$ chains with $N_{\text{L}} = 20$, 60, as well as $N_{\text{S}} = 20$ chains with $N_{\text{L}} =$ 60, 120. All melts contain 3000 monomers, except those with $N_{\text{L}} = 120$, which consist of 7200 monomers. The entanglement length N_{e} of the chains is difficult to estimate since different methods of calculating the entanglement length yield inconsistent results. Kremer and Grest[21] have done extensive simulations using this model and have estimated the entanglement length to be approximately 35 monomers, although this number varies from $20 \leq N_{\text{e}} \leq 60$. Thus, we expect our largest systems to contain entangled polymers. The blends consist of short polymer volume fractions of $\varphi_{\text{S}} = 0.1$, 0.5, and 0.9. Once the bimodal melt is prepared, it is further equilibrated to attain the new equilibrium state. A step strain of $\lambda_\alpha = 2.0$ is then implemented by affinely deforming the positions of the monomers in direction α, where $\alpha = x, y, z$ in turn. To ensure volume conservation, the monomer positions are compressed by a factor $1/\lambda^{1/2}$ in the remaining two directions. During the relaxation stage, polymer conformational properties are measured every 50 integration steps. The orientation of each bond with the direction of stretch is measured by the order parameter Q, as defined by eq 1. The end-to-end distance of each polymer in each direction is also measured, and the stress is calculated using the virial stress formula.[23,24] The shear relaxation modulus E, which measures the uniaxial component of the stress tensor, is calculated from the pressure tensor as

$$E = \frac{3}{2} \times \frac{P_{\alpha\alpha} - \text{Tr}\,P}{\lambda^2 - 1/\lambda} \tag{5}$$

where $P_{\alpha\alpha}$ is the value of the pressure tensor in the direction of stretch α. The pressure tensor itself is calculated in the following way:

$$P_{\alpha\alpha} = \frac{1}{V}\sum_i m v_{i\alpha}^{\,2} + \frac{1}{2V}\sum_{i\neq j}\frac{F_{ij,\alpha}}{r_{i\alpha} - r_{j\alpha}} \tag{6}$$

where $F_{ij,\alpha}$ is the α-component of the force applied by monomer j on monomer i. The simulations were performed on 12 Unix workstations as well as the IBM SP2 parallel computer of the Université de Sherbrooke. Our results are the average of a minimum of 1200 up to 15 000 polymers for each species and took well over 15 000 h of computer time.

The implementation of the step-strain method deserves some comment. Small affine deformation of up to $\lambda = 1.5$ can be performed on this system with little problem, since the equilibrium average distance between tethered monomers is approximately 0.97σ. However, the large deformation applied here necessarily extends the bonds beyond $R_0 = 1.5\sigma$, which results in

the potential energy U_T (see eq 3) being ill-defined. This problem is resolved in the following way. Immediately after the imposition of the step-strain, the parameter R_0 is increased in value from 1.5σ to 2.4σ, while simultaneously quenching the system to $T = 0$ and reducing the integration time step from $\delta t = 0.01\tau$ to 0.00005τ, where $\tau = \sigma(m/\epsilon)^{1/2}$ is the basic unit of time. The equations of motion are solved within a constant energy MD framework, with R_0 being progressively reduced until it returns to 1.5σ, after which δt is returned to its original value. During this procedure, there is some relaxation of the orientation and conformation of the polymers; however, the elapsed time for this period is the same amount of time that elapses between data collection points of the production runs. Furthermore, because this procedure is implemented at a low temperature, any relaxation is further minimized. Finally, we would like to point out that in most experiments there is in fact a delay between the stretching of the sample and the beginning of the data collection.[2] Although this delay is not long, on the order of 200 ms, it is often larger than the relaxation times of the short polymers. We chose such a large deformation because previous work[25] indicated that a larger deformation reduces the statistical fluctuations associated with the data collection.

III. Results and Discussion

Note that, unless otherwise noted, all systems are at a density of $\rho = 0.8$. Our results are presented in an order that stresses their meaning for the understanding of orientational coupling.

(A) The Order Parameter *Q* Relaxes More Slowly Than the End-to-End Distance *h*. We begin with two $N_S = 20$ and $N_L = 120$ bidisperse blends. The long-time behavior of the normalized orientation factor $Q_S(t)/Q_S(0)$ of the short polymer is shown in Figure 1 for volume fractions $\varphi_S = 0.1$ and $\varphi_S = 0.9$. These results clearly show that when the short polymer is the minority component, it remains oriented for a longer time than when it is the majority component, thus suggesting that it couples to the orientation of its environment. The short-time behavior (inset) shows a fast nonexponential decay for both concentrations. (See section J for more details on this part of the decay process.) This system represents the most entangled polymers, with the long polymers having approximately $N_L/N_e \approx 3.5$ entanglements in a $\varphi_L \rightarrow 1$ monodisperse melt. In Figure 2 we show the relaxation of the mean-square end-to-end distance of the short polymer, $\langle (h_S)^2 \rangle$, in both the parallel and transverse directions for $\varphi_S = 0.10$. These long-wavelength quantities return to their equilibrium isotropic values after a relaxation time $\tau_{hS} \approx 1400\tau$, while the bonds still show residual orientation up to at least $t = 2000\tau$ (Figure 1). For the $\varphi_S = 0.90$ blend, both the order parameter (Figure 1) and the mean-square end-to-end distances (not shown) return to their isotropic values at a time $\approx 800\tau$. Our model thus reproduces the local nature of the orientation coupling and the residual bond orientation seen in experiments. In the next few sections, we will be looking at various aspects of this apparent microscopic coupling in order to understand its nature and its importance.

(B) The Residual Orientation Is Due to the Environment. Although our data strongly imply that polymers couple orientationally to their environment, it is necessary to establish that the residual orientation

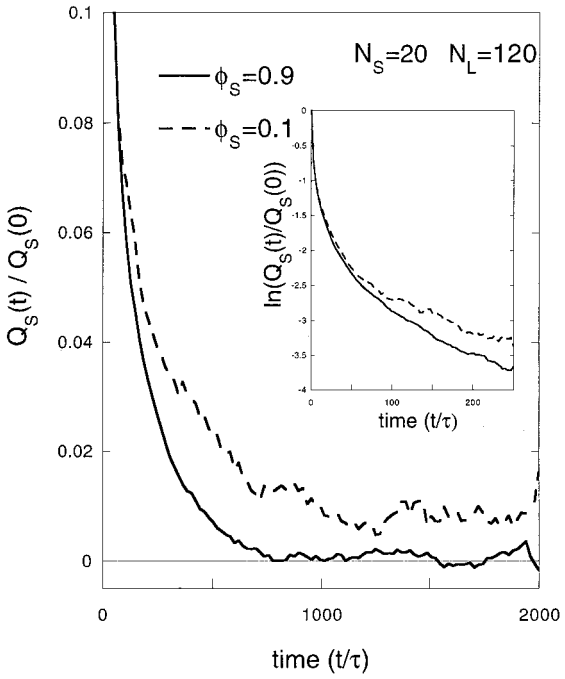

Figure 1. Reduced order parameter $Q_S(t)/Q_S(0)$ vs reduced time t/τ for short polymers of length $N_S = 20$ blended with long polymers of length $N_L = 120$. Two different volume fractions of short polymer are shown: $\varphi_S = 0.1$ (dotted line) and $\varphi_S = 0.9$ (solid line). Inset: this $\ln[Q_S(t)/Q_S(0)]$ vs time plot shows the rapid (and nonexponential) initial decay of the orientation. Note that the standard unit of molecular dynamics time is $\tau = \sigma(m/\epsilon)^{1/2}$.

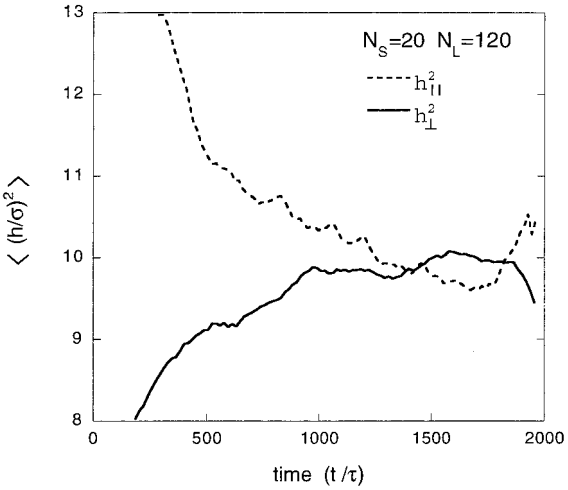

Figure 2. Reduced mean-square end-to-end distance $\langle (h/\sigma)^2 \rangle$ vs reduced time t/τ in the directions parallel (dotted line) and transverse (solid line) to the stretching direction for the $N_S = 20$, $N_L = 120$, and $\varphi_S = 0.1$ bidisperse blend. The axial and transverse components become equal at a time $\tau_{hS} \approx 1400\tau$, i.e., before the order parameter $Q_S(t)$ has decayed to zero (Figure 1), in agreement with experimental observations.[6,8]

of the short polymers is due solely to an oriented environment and not to other factors (such as various constraint release mechanisms) arising from the polydispersity of the system. Many authors[26−29] have proposed modifications of the standard Rouse or reptation descriptions to account for differences in dynamical constants arising in polydisperse melts. It is natural to expect the short (long) polymer to perceive greater (fewer) constraints in a bidisperse melt compared to the case of a monodisperse melt. To eliminate the possibility that the observed residual orientation of the short

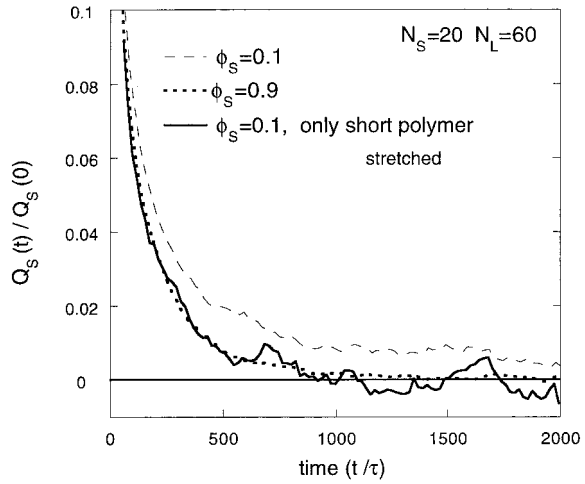

Figure 3. Reduced order parameter $Q_S(t)/Q_S(0)$ vs reduced time t/τ for short polymers of length $N_S = 20$ blended with long polymers of length $N_L = 60$. Three cases are shown: a $\varphi_S = 0.1$ system where both molecular species were stretched, a $\varphi_S = 0.1$ system where only the short polymers were stretched, and a $\varphi_S = 0.9$ system where both molecular species were stretched. The first one relaxes more slowly and keeps a residual orientation for an extended period of time, a clear proof that orientational coupling takes place.

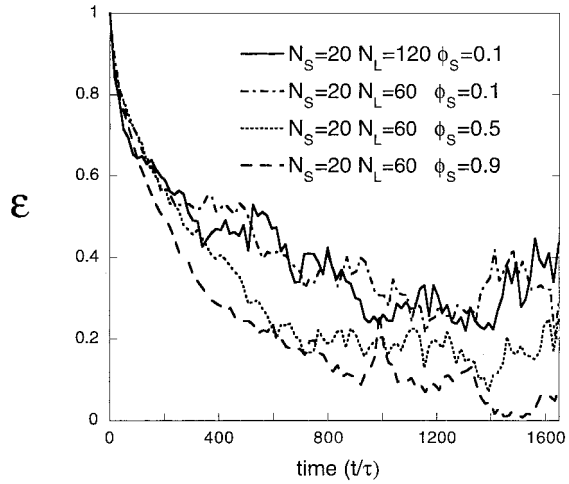

Figure 4. Coupling parameter $\epsilon = Q_S(t)/Q_L(t)$ vs reduced time t/τ for four different blends.

polymer when $\varphi_S = 0.10$ might be due to the mere presence of long polymers, we examined the following situation. In a $\varphi_S = 0.10$ blend of $N_S = 20$ and $N_L = 60$ chains, only the short polymers were stretched. (The long polymers were left in their original isotropic state.) In Figure 3, we compare this unusual situation to the physically realistic situation where both polymers are stretched. This comparison shows that there is residual orientation of the short polymers *only* when the environment is oriented. Although there are surely effects from polydispersity, the residual orientation is not such an effect. In fact, the relaxation of the short polymers in this artificial situation is essentially identical to its relaxation in a $\varphi_S = 0.90$ blend (Figure 3). We believe that this straightforward test demonstrates the existence of orientational coupling driven by steric interactions.

(C) The Coupling As Described by the Coupling Parameter ϵ. If the orientation of the short polymer is coupled to that of the long one, we can follow the time evolution of this coupling through the traditional empirical parameter defined as

$$\epsilon = Q_S/Q_L \tag{7}$$

We expect ϵ to be finite and time-dependent for short times since both polymers relax simultaneously but with different relaxation rates. However, this ratio is expected to decay toward zero for times larger than the normal (i.e., $\varphi_S = 1$) relaxation time of the short polymer. Figure 4 shows that this is not the case. For three of the blends shown here (i.e., for $\varphi_S \leq 0.5$), the parameter ϵ attains a plateau for long times. This means that the orientation of the short polymer becomes proportional to that of the long polymer, clearly indicating a direct coupling between the two. In other words, the short polymer is "waiting" for the long polymer to relax, and its residual orientation is thus due to the orientation of the long polymer. Of course, the noise increases for longer times because we are then dividing two small numbers. The data suggest that $\epsilon \approx 0.35 \pm 0.05$ when $\varphi_S = 0.10$, while we obtain $\epsilon \approx 0.18 \pm 0.05$ when $\varphi_S = 0.50$. In fact, the data show that N_L plays a minor role, if any (compare the two upper curves). However, the coupling parameter does depend on the volume fraction φ_S because the coupling is more important if the short polymers have more direct contacts with the long polymers in the blend. Indeed, the $\varphi_S = 0.90$ curve does not show a clear plateau and suggests a negligible degree of coupling when the long polymer is a small minority. Numerous authors have used ϵ as a measure of the strength of the effective "nematic" interactions in polymer blends. Our value agrees with that obtained by TBMM.[5] We want to stress again that this effective nematic interaction is purely steric because our intermolecular potential is purely repulsive. The dependence of the phenomenological parameter ϵ upon volume fraction φ_S will be studied in section F.

(D) The Coupling Parameter ϵ Increases with the Melt Density. As previously discussed, the earliest theoretical explanation for orientational coupling was based on a lattice theory of rubber[1] which found it favorable for self-avoiding free polymers to orient in an oriented medium. Given this argument, it is reasonable to expect the degree of steric interactions to have an effect on relaxation rates and the coupling parameter ϵ. In Figure 5 we display the relaxation of the reduced order parameter $Q_S(t)/Q_S(0)$ for a $N_S = 20$, $N_L = 60$, and $\varphi_S = 0.50$ blend at scaled densities of $\rho = 1.0$, 0.8, and 0.4. The relaxation times obviously increase substantially with density. However, these data cannot unequivocally indicate that steric effects alone account for this difference. Conformational and topological properties change with system density. For example, the end-to-end distance and the radius of gyration of the $N_S = 20$ polymer are both about 6% smaller in the higher density system. The decrease in the radius of gyration with increasing density is consistent with results from MD simulation by Smith et al.[32] They attributed the change in the end-to-end vector to a decrease in excluded volume with increasing density in accordance with screening effects. The entanglement length N_e was also found to decrease with an increase in the density. In comparison, these conformational parameters increase by about 9% in the low ($\rho = 0.4$) density system. Clearly, these small differences cannot explain the huge differences in relaxation rates between these systems.

The coupling parameter ϵ is shown in Figure 6 for these three systems. At low density, we cannot observe

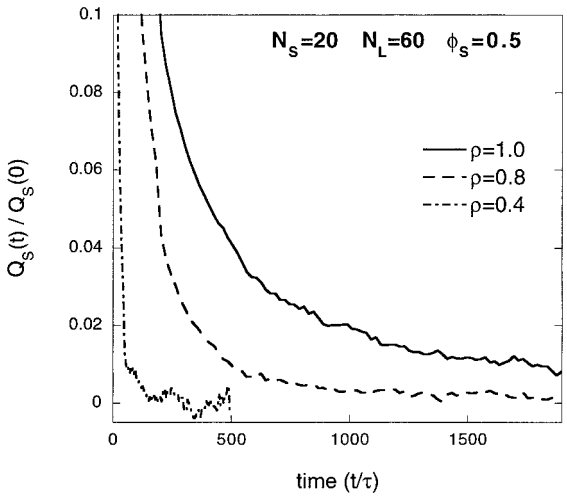

Figure 5. Reduced order parameter $Q_S(t)/Q_S(0)$ vs reduced time t/τ for short polymers of length $N_S = 20$ in a $\varphi_S = 0.50$ blend with long polymers of length $N_L = 60$. Three different (scaled) melt densities ($\rho = 0.4$, 0.8, and 1.0) are shown.

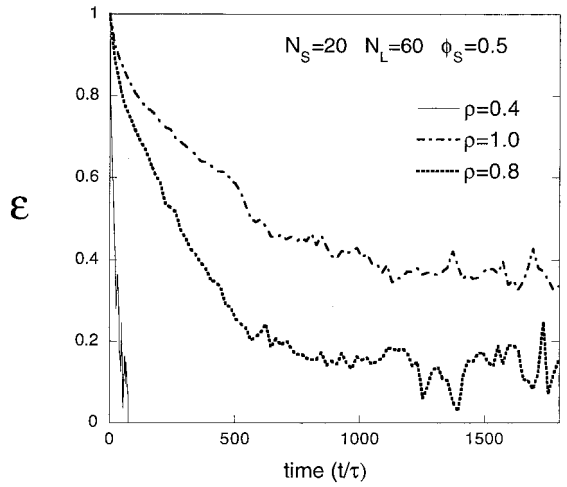

Figure 6. Coupling parameter $\epsilon = Q_S(t)/Q_L(t)$ vs reduced time t/τ for the three different blends described in Figure 5. Note that the coupling parameter is shown only for a short period of time for the $\rho = 0.4$ case because both the long and the short polymers relaxed to equilibrium very quickly.

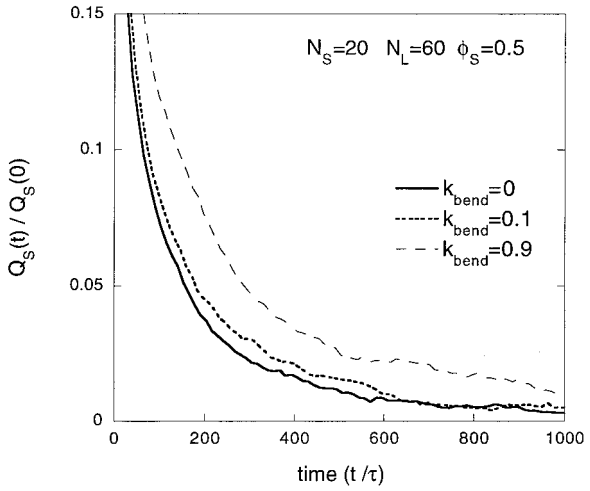

Figure 7. Reduced order parameter $Q_S(t)/Q_S(0)$ vs reduced time t/τ for short polymers of length $N_S = 20$ in a $\varphi_S = 0.50$ blend with long polymers of length $N_L = 60$. Three different polymer stiffnesses, as described by the bending coefficient k_{bend}, are shown. Stiffer polymers relax more slowly.

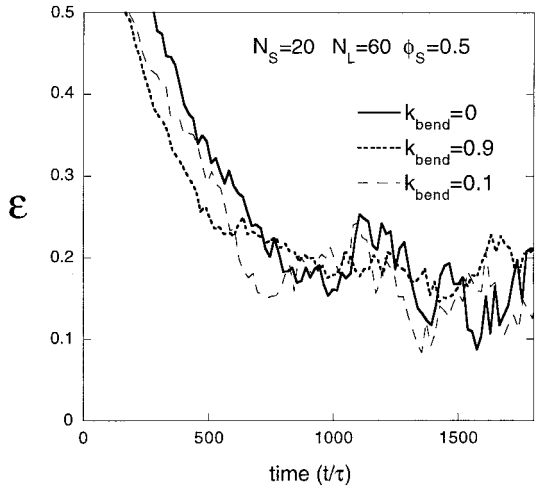

Figure 8. Coupling parameter $\epsilon = Q_S(t)/Q_L(t)$ vs reduced time t/τ for the three different systems described in Figure 7. In all three cases, the value of ϵ plateaus at $\approx 0.20 \pm 0.05$. No marked difference is observed with our data.

any plateau, and ϵ simply decays toward zero very quickly. Again, we observe that relaxation is slower for high-density systems. More interestingly, however, the plateau value of ϵ is clearly larger at higher densities, indicating that stronger orientational coupling is indeed produced by the increased steric interactions. In the case studied here, the orientational coupling parameter ϵ has approximately doubled, increasing from about $\epsilon = 0.18$ to about $\epsilon = 0.38$ when the density increased from $\rho = 0.80$ to $\rho = 1.0$, a remarkably large effect. The coupling parameter ϵ is thus related to both the number of oriented nearest-neighbor chains (sections C and F) and the local melt density.

(E) The Coupling Parameter ϵ Is the Same for Stiffer Polymers. Besides density, other physical parameters may have a direct impact on orientational coupling. One of them is the stiffness of the polymers (others include specific interactions between monomers of different species). We thus studied chain relaxation for molecules of different stiffness, where both polymers of a bidisperse melt had the same stiffness. Figure 7 shows once more that changing the microscopic molecular parameters directly affects the relaxation rates. Stiffer polymers relax more slowly than flexible ones. Here, the end-to-end distance of the stiffer polymers is 30% larger than those of the most flexible ones in equilibrium conditions. Compared to more flexible polymers, stiffer polymers tend to stay parallel to one another because chain packing costs less entropy. However, Figure 8 indicates that the orientational coupling parameter ϵ is not affected significantly when we increase polymer stiffness. In other words, both polymers are more oriented if they are stiffer, but direct coupling is similar. As far as we know, this result has not been observed nor predicted before. The fact that ϵ is essentially independent of chain stiffness suggests that orientational coupling is local. This will be studied further in section H. Of course, these results may not apply to a blend of polymers having different stiffness properties (or to block copolymers).

(F) The Relaxation Rates and the Coupling Parameter Depend on the Volume Fractions φ_S. Figure 1 showed that the relaxation rate of the short polymer depends on its volume fraction φ_S, while Figure 4 demonstrated that the coupling parameter ϵ was also a function of φ_S. In fact, the relaxation time of the long

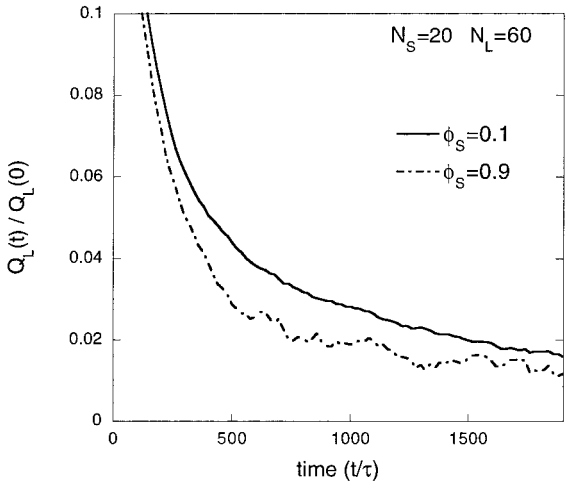

Figure 9. Reduced order parameter $Q_L(t)/Q_L(0)$ vs reduced time t/τ for two different volume fractions φ_S. The relaxation time of the long polymer is reduced when φ_S is increased, in agreement with experimental observations.[4]

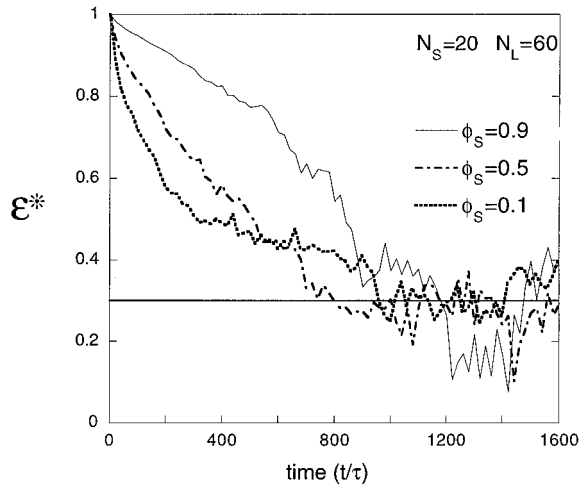

Figure 10. Intensive coupling parameter ϵ^* vs reduced time t/τ for different volume fractions of the $N_S = 20$ and $N_L = 60$ bidisperse blends. In all cases, the terminal plateau value is about the same.

polymer is also reduced if φ_S is increased (Figure 9). Such an effect has been observed by YKFP,[4] who reported that even a small increase in the number of short polymers greatly increased the relaxation rates. Of course, our model system cannot be directly compared to theirs because our polymer chains are so short that different dynamics governs their behavior. We were unable to follow the long chains until full relaxation due to limited computational resources.

Unfortunately, the coupling parameter ϵ, as defined by eq 7, does not take into account the fact that the total coupling between the short and long polymers must depend on their relative volume fractions. In other words, one must correct for volume fraction to obtain a coupling parameter ϵ^* that is an intensive (fieldlike) parameter. In a mean-field description of the coupling, the order parameter $Q_S(t)$ of the short polymers is coupled to the mean orientation field of the bulk as

$$Q_S(t) = \epsilon^*(\varphi_S Q_S(t) + \varphi_L Q_L(t)) \tag{8}$$

where $\varphi_L = 1 - \varphi_S$. Rewriting eq 8, we find that

$$\epsilon \equiv \frac{Q_S}{Q_L} = \frac{\epsilon^* \varphi_L}{1 - \epsilon^* \varphi_S} \tag{9}$$

This relationship between the extensive and intensive coupling parameters ϵ and ϵ^* was also suggested by TBMM.[5] Inverting eq 9, we obtain

$$\epsilon^* = \frac{\epsilon}{\varphi_L + \epsilon \varphi_S} \tag{10}$$

Note that we have $\epsilon^* \approx \epsilon$ when $\varphi_S \to 0$, as it should. In Figure 10, we plotted the intensive coupling parameter ϵ^* vs time t for the three different volume fractions shown in Figure 4 for a $N_S = 20$ and $N_L = 60$ bidisperse blend. All three systems show essentially the same plateau value of $\epsilon^* \approx 0.30 \pm 0.05$, demonstrating the validity of the concept of orientational coupling to the mean-field orientation of the bulk. Of course, the noise is more important for $\varphi_S = 0.90$ because the total coupling is weak when the short polymer is the majority. Interestingly, although all three decays appear to converge toward the same plateau, the decays are quite different. The short time decay curves are either concave ($\varphi_S = 0.1$), approximately linear ($\varphi_S = 0.5$), or convex ($\varphi_S = 0.9$), depending on the volume fraction φ_S.

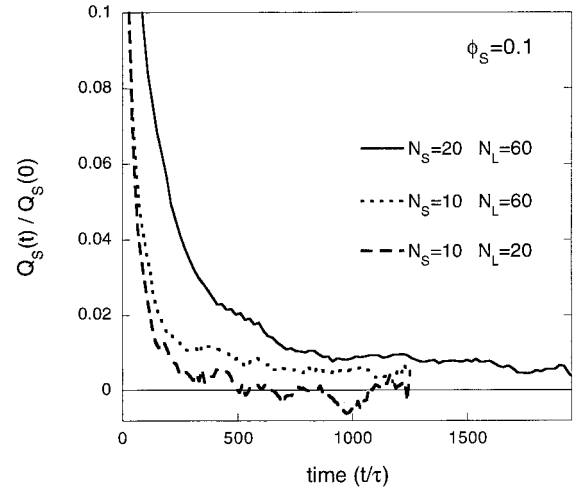

Figure 11. Reduced order parameter $Q_S(t)/Q_S(0)$ vs reduced time t/τ for various combinations of short and long polymers, as indicated. The volume fraction of short polymer is $\varphi_S = 0.1$ in all cases.

(G) The Chain Lengths $N_{S,L}$ Affect the Relaxation Rates. It is reasonable to expect that the chain lengths will affect the relaxation rates since they affect all other dynamical processes. This has indeed been seen experimentally by TBMM.[5] The bulk relaxation occurs in two clear steps. Initially there is a fast relaxation of both polymers. During this stage, the short polymer releases constraints on the longer polymer, and it would reach an isotropic relaxed state if it were not for orientational coupling. (This is, of course, what happened when we stretched only the short polymers; see Figure 3.) At longer times, the relaxation rate is determined by the long polymer, to which the short polymer is orientationally coupled. One anticipates that at fixed volume fraction the relaxation of the shorter polymer would occur faster when both N_S and N_L are smaller. For $\varphi_S = 0.1$, this relaxation is shown in Figure 11. Our results are consistent with those of TBMM.[5] Similarly, the relaxation time of the long polymer increases with N_S (Figure 12).

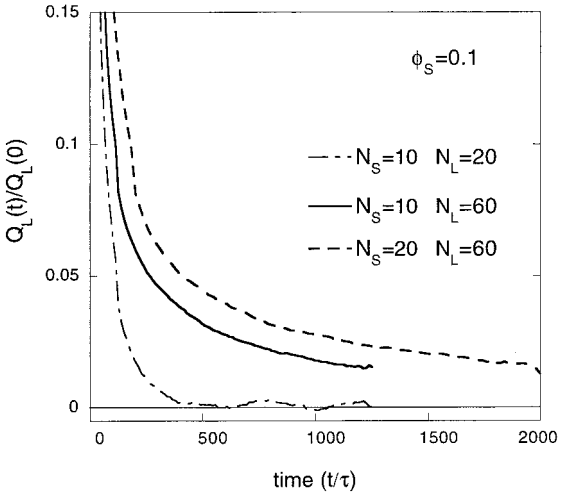

Figure 12. Reduced order parameter $Q_L(t)/Q_L(0)$ vs reduced time t/τ for various combinations of short and long polymers, as indicated. The volume fraction of short polymer is $\varphi_S = 0.1$ in all cases.

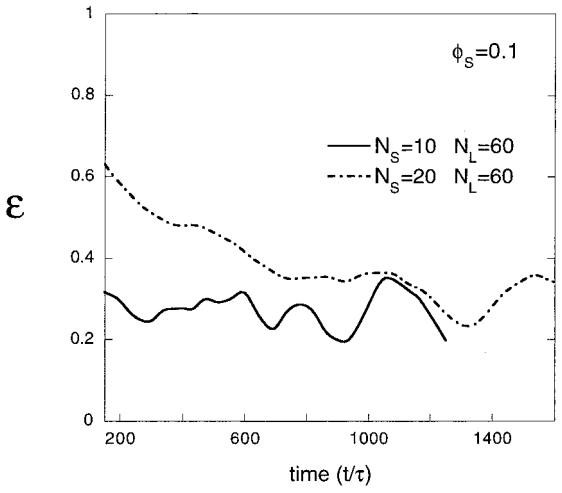

Figure 13. Coupling parameter $\epsilon = Q_S(t)/Q_L(t)$ vs reduced time t/τ for two different lengths of short polymer $N_S = 10$, 20 each blended with $N_L = 60$, at $\varphi_S = 0.1$. The data for $N_S = 10$ was too noisy for times larger than 1200.

In Figure 4, we saw that ϵ was little affected when N_L was increased from 60 to 120 (with $N_S = 20$ and $\varphi_S = 0.1$). This is evidence that orientational coupling is a local process. Further evidence of orientational coupling from a local process is shown in Figure 10 where the system changes from an unentangled melt at $\varphi_S = 0.1$ to an entangled melt at $\varphi_S = 0.9$, and the coupling parameter ϵ^* remains unaffected for times $t/\tau > 800$. The situation is qualitatively different, however, when N_S is very small. For example, Figure 13 suggests that the plateau value of ϵ is somewhat lower for very small values of N_S. This reason for this somewhat unexpected effect will be discussed in the next section.

(H) The Orientation of Different Polymer Subchains. To understand why very short polymers appear to be less affected by orientational coupling, we studied the relaxation of selected subsections of the short polymer chains for two $N_S = 20$ and $N_L = 60$ polymer blends. The short-time relaxation of the orientation of the four-bond subchains in the middle and at the ends of the $N_S = 20$ chain are shown in Figure 14A. Not surprisingly, the end segment of the chain relaxes at a faster rate than the middle segment, for both volume

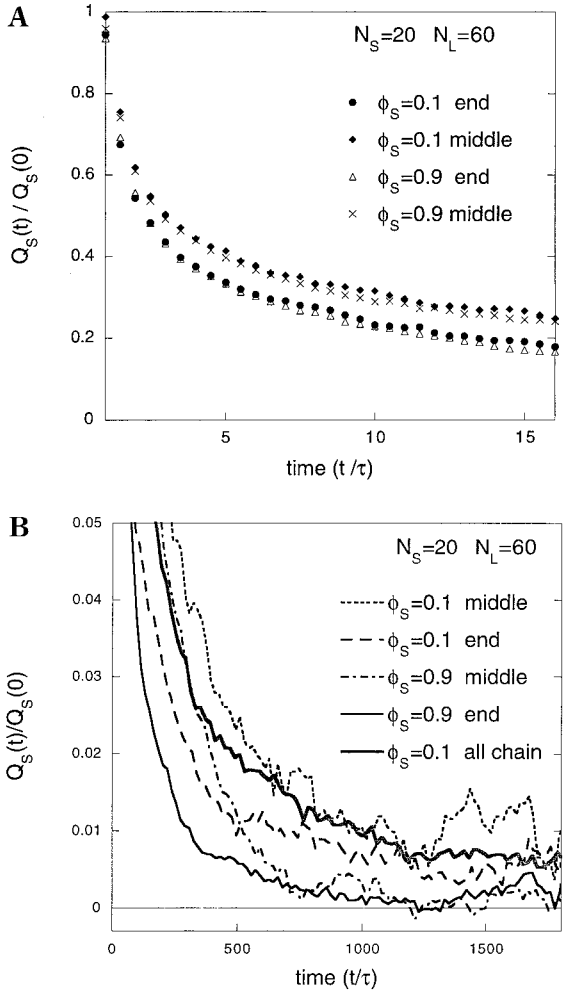

Figure 14. Reduced order parameter $Q(t)/Q(0)$ vs reduced time t/τ for the middle and end subchains of the short polymer molecules in two $N_S = 20$ and $N_L = 60$ bidisperse blends: (A) short times; (B) long times. The global order parameter of the $N_S = 20$ chain is included for $\varphi_S = 0.1$.

fractions φ_S studied. The effects of φ_S are seen remarkably early on, i.e., for times $t < 10\tau$, as marked by a slight difference in relaxation rates.

The long-time relaxation of the short polymer is shown in Figure 14B for the same systems. When the short polymer is the majority species ($\varphi_S = 0.9$), the relaxation of both the middle and the end subchains occurs smoothly. Although the middle subchains always retain more orientation than the end ones, both curves converge toward $Q_{S,middle} = Q_{S,ends} = 0$ at $t \approx 1200\tau$. Yet, when the short polymer is the minority species ($\varphi_S = 0.1$), the subchain relaxation is qualitatively different. The subchains relax smoothly until about $t = 500\tau$, with the middle subchains again retaining more orientation than the end subchains. For times $t > 500\tau$, however, both relaxation curves change fairly abruptly. Although both orientations decay much more slowly after this time, the middle subchain does retain more orientation than the end subchains for a long period of time. In other words, the effective coupling constant ϵ appears to be larger for the middle part of the chain. Also shown is the decay curve given in Figure 3 for the global order parameter Q_S; clearly, this curve is situated between the other two curves. Therefore, there is a strong end-of-the-chain effect. This explains the smaller value of ϵ found for $N_S = 10$ in the previous section since this short

molecule is essentially two end subchains of four bonds each connected together.

(I) The Stress−Optical Law. This calculation based on eq 5 is used primarily to ensure that the stress−optical law holds, as predicted by various analytical models of orientational coupling.[14,17] In Figure 15, we show that the $Q_{bulk}(t)$ vs $E(t)$ curve is well-described by a straight line of slope 1, indicating that these two properties are indeed proportional to one another during the entire relaxation process. This is in agreement with the experimental findings of YKFP[4] and the simulation work of Gao and Weiner.[20] Similar relationships were found in all cases we studied via NEMD. Therefore, our model does satisfy the stress−optical law, which implies that the simulations are still in a linear viscoelastic regime and that the stretch imposed on the system was not so large that a comparison to experiment was rendered meaningless.

(J) The Short Time Relaxation. The main goal of this study was to develop a NEMD computer simulation model to study the long-time relaxation properties of bidisperse polymer blends (and, eventually, of miscible blends of dissimilar polymers). However, the short-time dynamics are not without interest. Our systems start very far from equilibrium since the stretching factor is $\lambda = 2.0$. Therefore, the initial (fast) phase of the relaxation process is very complicated and strongly nonexponential (see, e.g., inset of Figure 1). We have examined this part of the relaxation process in order to find (1) a simple analytical form that can be used to fit the decay curves and (2) quantitative estimates of the relevant time scales. Of course, such decay curves can easily be fitted using a sum of several exponentials, but such fits do not necessarily clarify the problem at hand.

Two methods can be used to associate a time scale for the early relaxation process. First, one can try to fit the data (or at least a large part of it) with a mathematical form

$$\frac{Q(t)}{Q(0)} = f\left(\frac{t}{\tau_{Qf}}\right), \quad \text{where } f(0) = 1 \text{ and } f(t\rightarrow\infty) = 0 \qquad (11)$$

The time τ_{Qf} then provides a natural time scale to describe the relaxation. Alternatively, the following equation is often used to obtain an empirical (integral) relaxation time:

$$\tau_{Qi} = \int_0^\infty \frac{Q(t)}{Q(0)}\,dt \qquad (12)$$

The two methods give identical results if $f(t/\tau_{Qf}) = \exp(-t/\tau_{Qf})$. While eq 12 is easy to implement and objective, eq 11 requires one to choose both a mathematical form $f(x)$ and possibly a range of times over which this function is assumed to describe the data in a satisfactory way. Moreover, the relaxation times obtained from eq 11 can only be compared if the mathematical form $f(x)$ remains strictly identical for all the systems under study.

Figure 16 shows that stretched exponentials $f(x) \sim \exp(-x^\mu)$ provide an excellent fit to the relaxation data for both polymers in a $\varphi_S = 0.1$ blend. Similar results were observed with all the other systems, and the stretched exponents μ were in the range 0.18−0.45. Therefore, we can characterize the decay curves by two numbers: the stretched exponent μ and the integral relaxation time τ_{Qi}. Our data are shown in Table 1 for all the systems that we studied. Note that τ_{Qf} is related to these two numbers via the equation $\tau_{Qf} = \mu\tau_{Qi}/\Gamma(1/\mu)$. We remark that the exponents μ_S are systematically larger for larger volume fractions φ_S, while the exponents μ_L are fairly insensitive to the volume fraction. Moreover, it is clear that $\mu_S > \mu_L$. As for the molecular size dependence of the relaxation times, the data of Table 1 lead to the empirical relation $\tau_{Qi,L}/\tau_{Qi,S} \sim (N_L/N_S)^{1.10\pm0.04}$. Finally, as expected, the relaxation times decrease when the volume fraction φ_S increases, although this dependence is rather weak for the $N_S = 10$

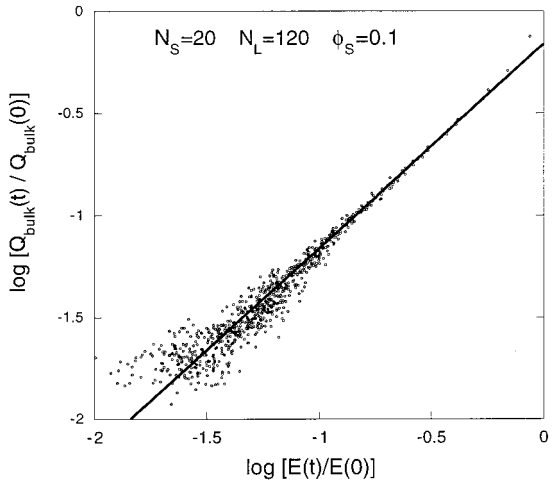

Figure 15. Reduced order parameter $Q_{bulk}(t)/Q_{bulk}(0)$ vs reduced shear relaxation modulus $E(t)/E(0)$ for $N_S = 20$, $N_L = 60$ at $\varphi_S = 0.1$. All blends showed a similar linear behavior.

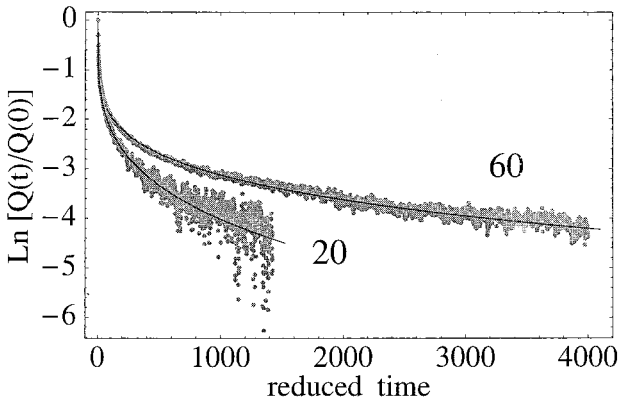

Figure 16. Ln[$Q(t)/Q(0)$] vs scaled time t/τ for the short and long polymers in a $N_S = 20$, $N_L = 60$, and $\varphi_S = 0.10$ bidisperse blend. The solid lines give the best fits: $y = -(t/90)^{0.27}$ for $N_S = 20$ and $y = -(t/340)^{0.21}$ for $N_L = 60$.

Table 1. Data Obtained from Stretched Exponential Fits of the Decay Curves of the Reduced Order Parameter $Q(t)/Q(0)$[a]

N_S	N_L	φ_S	μ_S	μ_L	$\tau_{Qi,S}$	$\tau_{Qi,L}$
10	20	0.10	0.47	0.34	15	34
		0.50	0.43	0.34	15	31
		0.90	0.45	0.36	14	27
10	60	0.10	0.28	0.22	29	200
		0.50	0.33	0.23	18	150
		0.90	0.44	0.24	14	87
20	60	0.10	0.27	0.21	90	340
		0.50	0.31	0.22	65	250
		0.90	0.35	0.25	55	160
20	120	0.10	0.25	0.19	100	650
		0.90	0.33		53	

[a] The times are given in units of the MD time τ. The errors on the values quoted here are approximately ±15% or less.

and $N_L = 20$ case. Models of relaxation processes with mode−mode coupling indicate that small exponents μ are related to strong cooperativity during the relaxation.[30,31] This is not an unexpected result in a system where the far-from-equilibrium molecular populations are strongly coupled via entanglements, excluded-volume interactions, and orientational effects. Another interpretation is that stretched exponentials simply represent a convenient way to express a sum of exponentials, where the latter is the result of a description that takes into account the different rates of relaxation of identical polymer chains in such a disordered (heterogeneous) system.[33,34]

IV. Summary

Extensive NEMD simulations were used to study orientation coupling in bidisperse polymer melts. Since orientational coupling has been well documented in many experiments, the focus of this work was first to ensure that our computer model could reproduce (at least qualitatively) experimental results and then to carry out a systematic investigation of the nature of this coupling. The short polymers were always smaller than the entanglement length while the long polymers ranged from below to above the entanglement. Unconnected monomers interacted only through a repulsive (steric) potential, and the relaxation of the bond orientation and end-to-end distance of both the long and short polymers was monitored and studied in detail.

Experimentally, it is found that after a step strain the rate of relaxation of both long and short polymers is inversely proportional to the volume fraction $\varphi_L = 1 - \varphi_S$ of long polymers in the melt,[4] a result that our simulations reproduced for all the blends. The relaxation of the orientation of the short polymer happens in two steps. There is an initial fast decay toward equilibrium; when the short polymer is the majority component, this fast decay smoothly attains the isotropic value of the orientation. However, when the short polymer is the minority component, a nonzero residual orientation is maintained for a surprisingly long period of time. This is a clear indication of the polymer coupling to its anisotropic environment. These results are consistent with calculations[1] which show that steric effects alone make it entropically favorable for a probe polymer to become oriented when placed in an oriented environment. Simulations with the long polymer left in its isotropic state also demonstrated that residual orientation was caused by orientational coupling and not merely by the presence of long polymers. We conclude that the residual orientation that is observed is due to a coupling of the short polymer to an oriented environment and that this coupling is mediated by steric interactions and occurs even in the absence of entanglements. Orientational coupling, normally absent from theoretical models, is thus an important effect to consider whenever two miscible polymers having different intrinsic relaxation rates are blended. The local nature of the coupling is seen in the present model, where the end-to-end distance of the short polymers in directions parallel and transverse to the imposed stretch return to their equilibrium values while the bonds are still locally orientated. This is consistent with experiments.[6,8] Finally, the relaxation process was observed to satisfy the stress−optical law despite the existing orientational coupling.

A convenient way of measuring the degree of orientational coupling is through the parameter ϵ^* defined by eq 7. If we consider ϵ^* to be the mean-field coupling between any given polymer and its oriented environment, our simulations indicate that at a density of $\rho = 0.8$ the coupling is the same for all volume fractions ($\epsilon^* \approx 0.30 \pm 0.05$), hence validating the concept of a "mean molecular orientational field". Experimentally,[4] this coupling parameter has been found in the range 0.1−1.0. Further simulations of somewhat stiffer polymers showed that the orientational coupling parameter was essentially unchanged although the relaxation was greatly slowed by the additional polymer stiffness. Since these simulations were done on chemically identical polymers, we conclude that stiffness alone does not change the degree of orientational coupling. However, increasing the density of the system to $\rho = 1.0$ almost doubled the degree of orientational coupling, while decreasing to $\rho = 0.4$ gave no significant coupling. The dramatic change in ϵ (or ϵ^*) as a function of the density (or, equivalently, the degree of excluded-volume interactions) leads us to conclude that steric interactions, at least for short chains, dominate the orientational coupling.

The mean-field nature of the orientational coupling was further studied by looking at subchains. Not surprisingly, the orientation of the end segments of the short chains relax faster than that of the middle segments because they enjoy more freedom. As a consequence, the residual orientation of the end segments is lower when the coupling to the orientation of the long polymers dominates the problem. However, it is clear that both the middle and end segments must be coupled to the same mean "bulk" orientational field. The situation is thus similar to that of a spin in a local field ϵ^*. The mean orientation of the spin depends on ϵ^*, of course, but also on the local temperature. The higher the temperature, the lower the resulting spin orientation. In our case, the dynamic freedom of the end segments is equivalent to a higher temperature, hence the lower orientation that results from the coupling to the mean field ϵ^*. Consequently, the global orientation of the short polymers contains these end effects, but the latter become negligible for large enough polymers. It seems to us that this unavoidable finite-size effect has been neglected in most if not all experimental studies. It would indeed be quite interesting to selectively label certain parts of the chains in order to understand the contribution of the different parts of the molecule to orientational coupling.

We also studied the time dependence of our far-from-equilibrium relaxation process to see whether it could be described using simple mathematical expressions. Satisfactory fits were obtained with stretched exponentials $\exp[-(t/\tau_Q)^\mu]$, with μ in the range 0.18−0.45. For short times $t < \tau_Q$, this leads to extremely fast dynamics. However, the small values of μ mean that the long-time relaxation is actually quite slow. Interestingly enough, the integral relaxation times τ_{Qi} were found to scale roughly like N^1 for all the systems under study, regardless of volume fractions and molecular sizes.

The success of this computer model in reproducing experimental results and obtaining insights into the nature of the origin of orientational coupling encourages us to use it to explore orientational coupling in other miscible polymer blends. Our finding that the end segments can play an important role, for example, suggests that ABA triblock copolymers with stiffer end blocks should be more affected by orientational coupling

than BAB triblocks with flexible end blocks. Other polymer structures, such as ring chains and branched molecules, must also show different coupling properties. Mixtures of flexible and stiff polymers should be quite interesting since we found that the coupling parameter ϵ^* is not affected by polymer stiffness if *both* polymers share the same bending potential. Finally, the main long-term goal is to study blends of dissimilar but miscible polymers. In this case, the necessary specific interactions between dissimilar monomers should lead to local density fluctuations that will directly affect the mean orientational field of the bulk.

Acknowledgment. The authors thank Robert Prud'homme, Michel Pézolet, Géraldine Bazuin, and Marc Pépin for fruitful discussions. This work was supported by a Collaborative Project Grant from the National Science and Engineering Research Council of Canada. We also acknowledge the use of the Université de Sherbrooke's IBM SP2 multiprocessor UNIX computer.

References and Notes

(1) DiMarzio, E. A. *J. Chem. Phys.* **1962**, *36*, 1563.
(2) Ylitalo, C. M.; Zawada, J.; Fuller, G. G.; Abetz, V.; Stadler, R. *Polymer* **1992**, *33*, 2949.
(3) Kornfield, J. A.; Fuller, G. G.; Pearson, D. S. *Macromolecules* **1989**, *22*, 1334.
(4) Ylitalo, C. M.; Kornfield, J. A.; Fuller, G. G.; Pearson, D. S. *Macromolecules* **1991**, *24*, 749.
(5) Tassin, J.-F.; Baschwitz, A.; Moise, J.-Y.; Monnerie, L. *Macromolecules* **1990**, *23*, 1879.
(6) Brereton, M. G. *Macromolecules* **1993**, *26*, 1152.
(7) Brereton, M. G.; Ries, M. E. *Macromolecules* **1996**, *29*, 2644.
(8) Sotta, P.; Deloche, B.; Herz, J.; Lapp, A.; Durand, D.; Rabadeux, J.-C. *Macromolecules* **1987**, *20*, 2769.
(9) Treloar, L. *The Physics of Rubber Elasticity;* Oxford University Press: Oxford, U.K., 1967.
(10) Boue, F.; Farnoux, B.; Bastide, J.; Lapp, A.; Herz, J.; Picot, Cl. *Europhys. Lett.* **1986**, *1*, 637.
(11) Doi M.; Edwards, S. F. *The Theory of Polymer Dynamics*; Clarendon: Oxford, U.K., 1986.
(12) Tanaka, T.; Allen, G. *Macromolecules* **1977**, *10*, 426.
(13) Fukuda, T.; Takada, A.; Miyamoto, T. *Macromolecules* **1991**, *24*, 6210.
(14) Jarry, J.-P.; Monnerie, L. *Macromolecules* **1979**, *12*, 316.
(15) Doi, M.; Watanabe, H. *Macromolecules* **1991**, *24*, 740.
(16) Merrill, W. W.; Tirrel, M.; Tassin, J.-F.; Monnerie, L. *Macromolecules* **1989**, *22*, 896.
(17) Doi, M.; Pearson, D. S.; Kornfield, J.; Fuller, G. *Macromolecules* **1989**, *22*, 1488.
(18) Gao, J.; Weiner, J. H. *Macromolecules* **1988**, *21*, 773.
(19) Gao, J.; Weiner, J. H. *J. Chem. Phys.* **1995**, *103*, 1614.
(20) Gao, J.; Weiner, J. H. *Macromolecules* **1996**, *29*, 6048.
(21) Kremer, K.; Grest, G. *J. Chem. Phys.* **1990**, *92*, 5057.
(22) Allen, M. P.; Tildesley, D. J. *Computer Simulations of Liquids*; Clarendon: Oxford, U.K., 1987.
(23) Gao, J.; Weiner, J. H. *Macromolecules* **1987**, *20*, 2520.
(24) Everaers, R.; Kremer, K.; Grest, G. S. *Macromol. Symp.* **1995**, *93*, 53.
(25) Barsky, S.; Plischke, M.; Joós, B.; Zhou, Z. *Phys. Rev. E* **1996**, *54*, 5370.
(26) Doi, M.; Graessley, W. W.; Helfand, E.; Pearson, D. S. *Macromolecules* **1987**, *20*, 1990.
(27) Hess, W. *Macromolecules* **1987**, *20*, 2587.
(28) Herman, M. F. *Macromolecules* **1992**, *25*, 4931.
(29) Colby, R. H. *J. Phys. II (Paris)* **1997**, *7*, 93.
(30) Ngai, K. L.; Rajagopal, A. K.; Teitler, S. *J. Chem. Phys.* **1988**, *88*, 5086.
(31) Palmer, G. G.; Stein, D. L.; Abrahmas, E.; Anderson, P. W. *Phys. Rev. Lett.* **1984**, *53*, 958.
(32) Smith, S. W.; Hall, C. K.; Freeman, B. D. *J. Chem. Phys.* **1996**, *104*, 5616.
(33) Heuer, A.; Okun, K. *J. Chem. Phys.* **1997**, *106*, 6176.
(34) Kaatz, P.; Pretre, P.; Meir, U.; Stalder, U.; Brosshard, C.; Gunter, P.; Zysset, B.; Stauhelin, M.; Ahlheim, M.; Lehr, F. *Macromolecules* **1996**, *29*, 1666.

MA971826X